Electronic Supplementary Material (ESI) for Journal of Materials Chemistry A.

Supporting Information

Highly Selective Photothermal Conversion of CO_2 to Ethylene Using Hierarchical Boxwood Ball-like Weyl Semimetal WTe_2 Catalysts

Xiaoyue Zhang,[a] Chaoran Dong,[a] Yong Yang, [b,*] Yingjie Hu,[c] Lizhi Wu,[b] Yu Gu,[d] Kan Zhang,[d] Jinyou Shen [a,*]

[a] Key Laboratory of Environmental Remediation and Ecological Health, Ministry of Industry and Information Technology, School of Environmental and Biological Engineering, Nanjing University of Science and Technology, Nanjing 210094, China

[b] School of Chemistry and Chemical Engineering, Nanjing University of Science and Technology, Nanjing 210094, China

[c] Nanjing Key Laboratory of Advanced Functional Materials, Nanjing Xiaozhuang University, Nanjing 210094, China.

[d] MIIT Key Laboratory of Advanced Display Material and Devices, School of Materials Science and Engineering, Nanjing University of Science and Technology, 210094, Nanjing, China.

*Corresponding authors. E-mail addresses: yychem@njust.edu.cn (Y. Yang), shenjinyou@mail.njust.edu.cn (J. Shen).

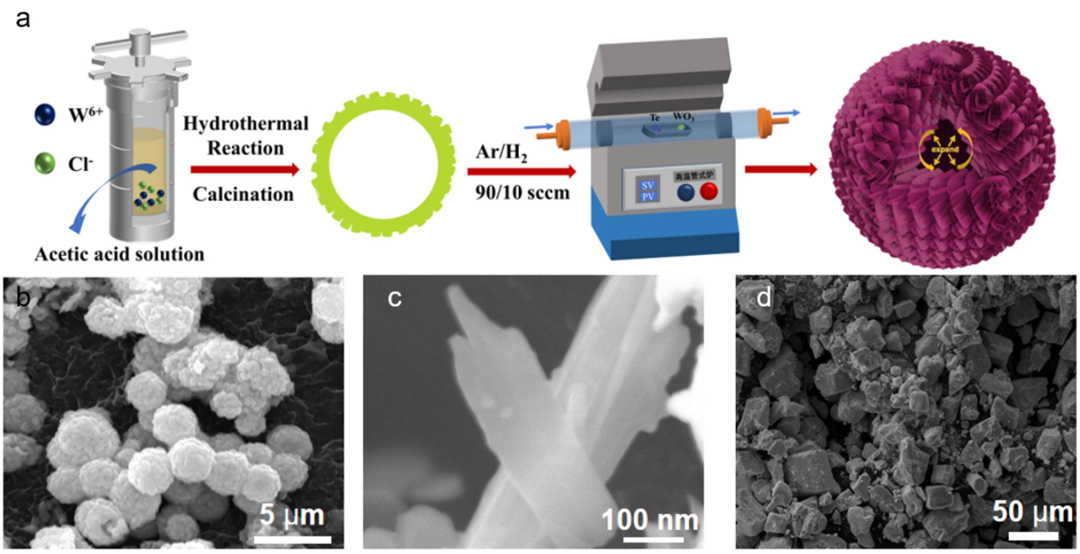

Fig. S1 (a) Illustration of the synthesis of the 3D WTe_2 HNSs; FE-SEM images of (b) WTe_2 HNSs; (c) WTe_2 NRs, d. WTe_2 NPs.

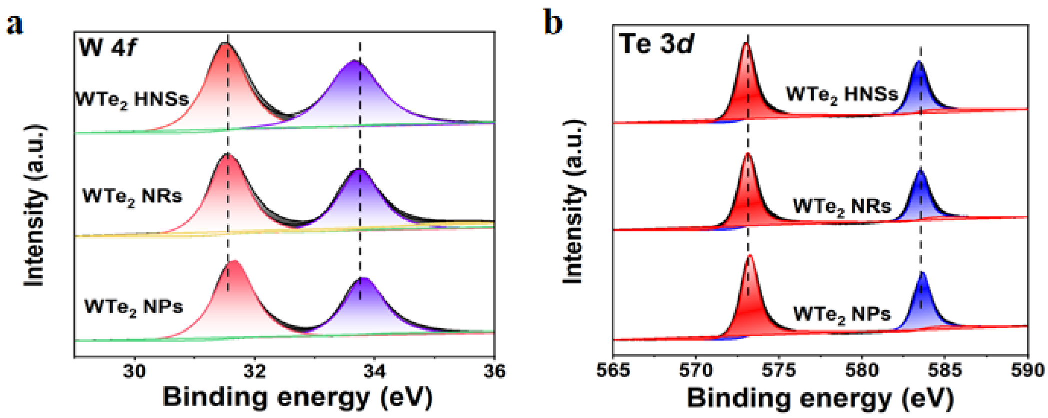

Fig. S2 XPS survey spectra of WTe_2 HNSs, WTe_2 NRs, WTe_2 NPs; (a) W 4*f* and (b)Te 3*d*, respectively.

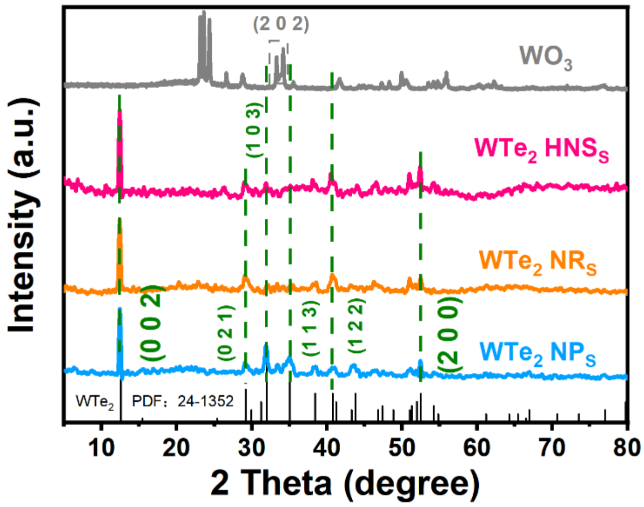

Fig. S3 XRD patterns of WO_3, WTe_2 HNSs, WTe_2 NRs and WTe_2 NPs.

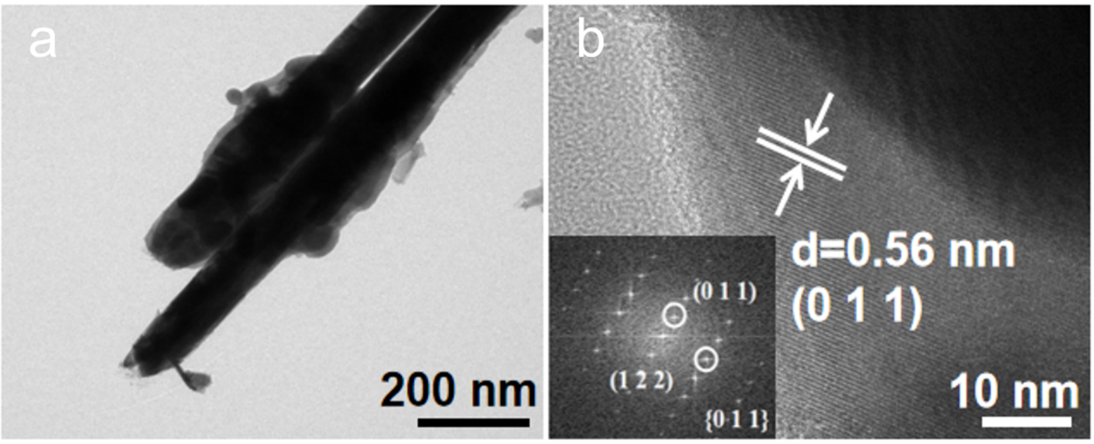

Fig. S4 (a) The TEM image and (b) HRTEM image of WTe_2 NRs**.**

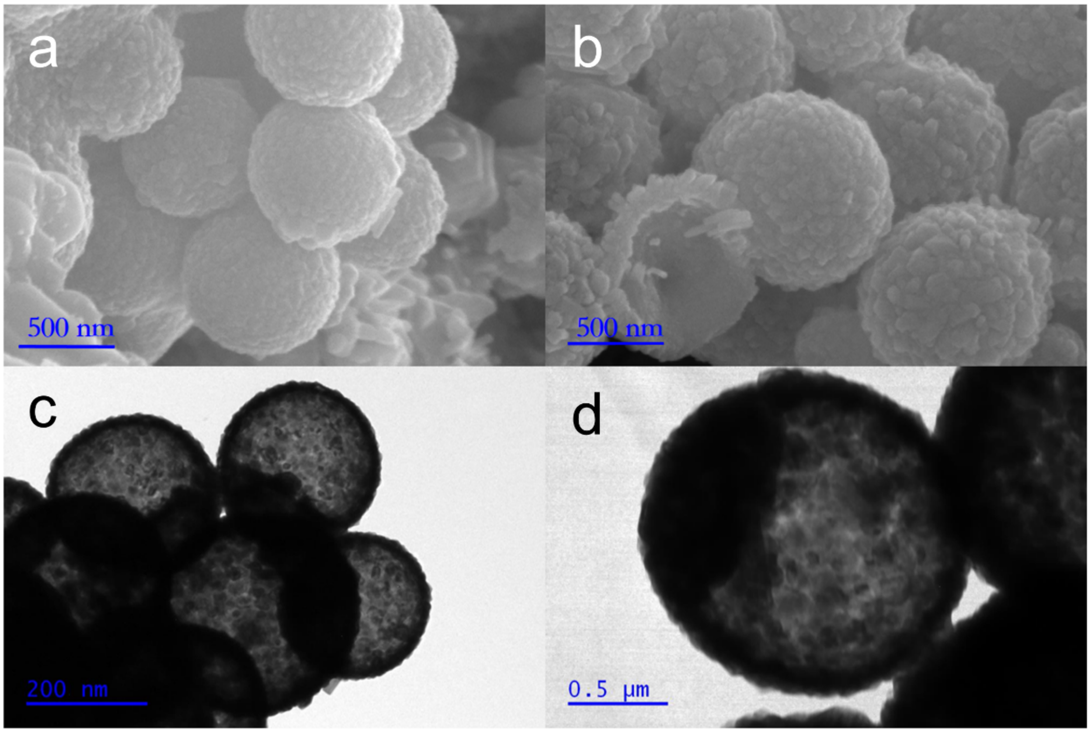

Fig. S5 FE-SEM images and the whole TEM image of WO_3.

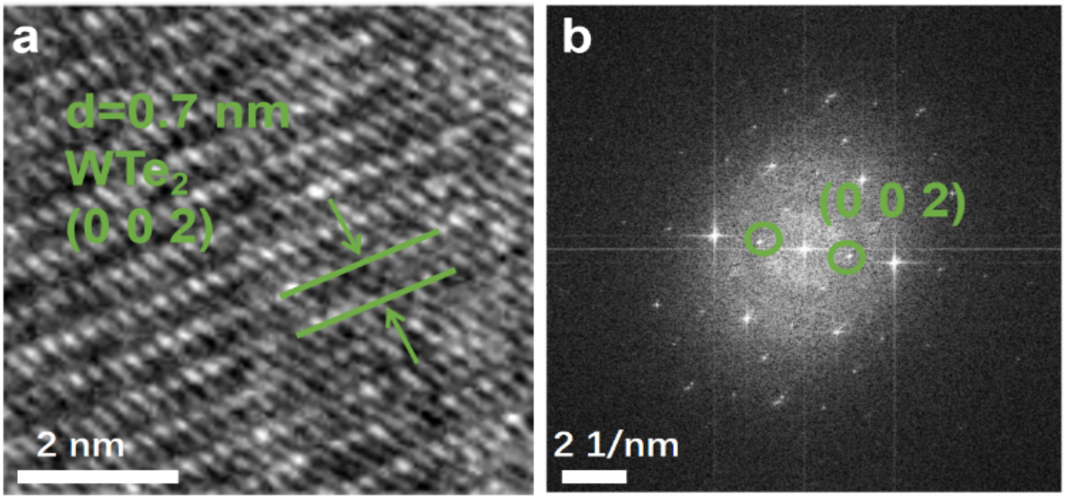

Fig. S6 (a) HAADF STEM image of WTe_2 HNSs; (b) SAED patterns showing polycrystalline nanomaterials.

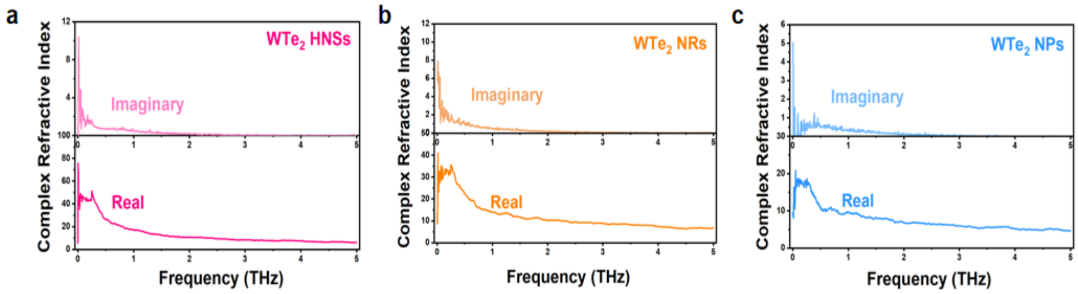

Fig. S7 (a-c) Real and imaginary images of refractive index of WTe_2 HNSs, NRs and NPs samples.

Complex refractive index

See also: Mathematical descriptions of opacity.

When light passes through a medium, some part of it will always be absorbed. This can be conveniently taken into account by defining a complex refractive index,

$\underline{n}=n + ik$.

Here, the real part *n* is the refractive index and indicates the phase velocity, while the imaginary part *k* is called the optical extinction coefficient or absorption coefficient.

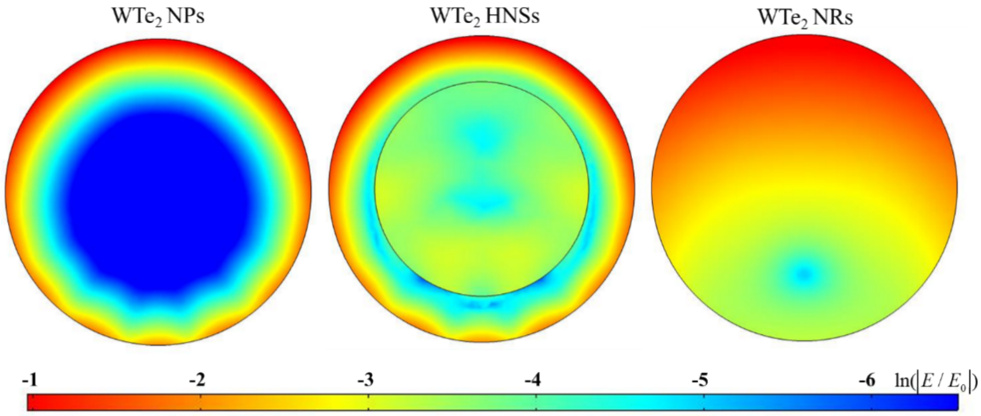

Fig. S8 Simulated electric field distribution of WTe_2 HNSs, NRs and NPs under 450 nm light of WTe_2 HNSs, NRs and NPs samples.

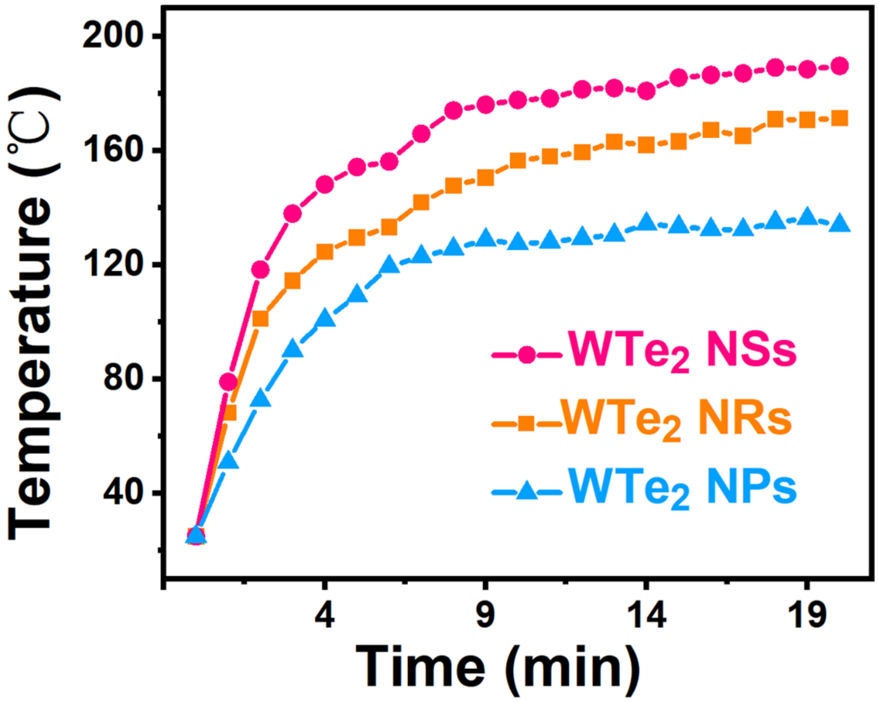

Fig. S9 The temperature curves of different samples under Xe lamp light.

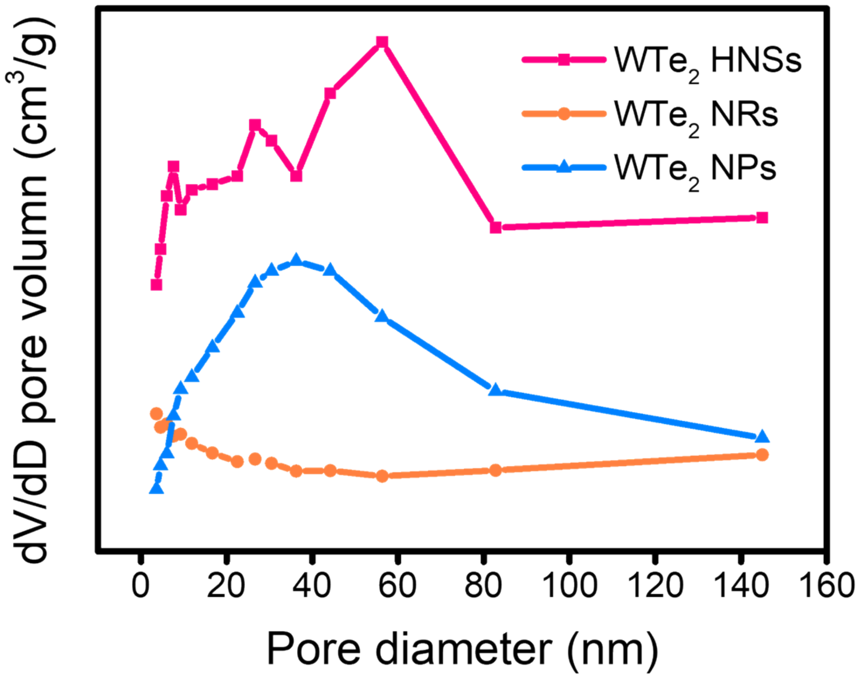

Fig. S10 Pore size distribution curves of different samples.

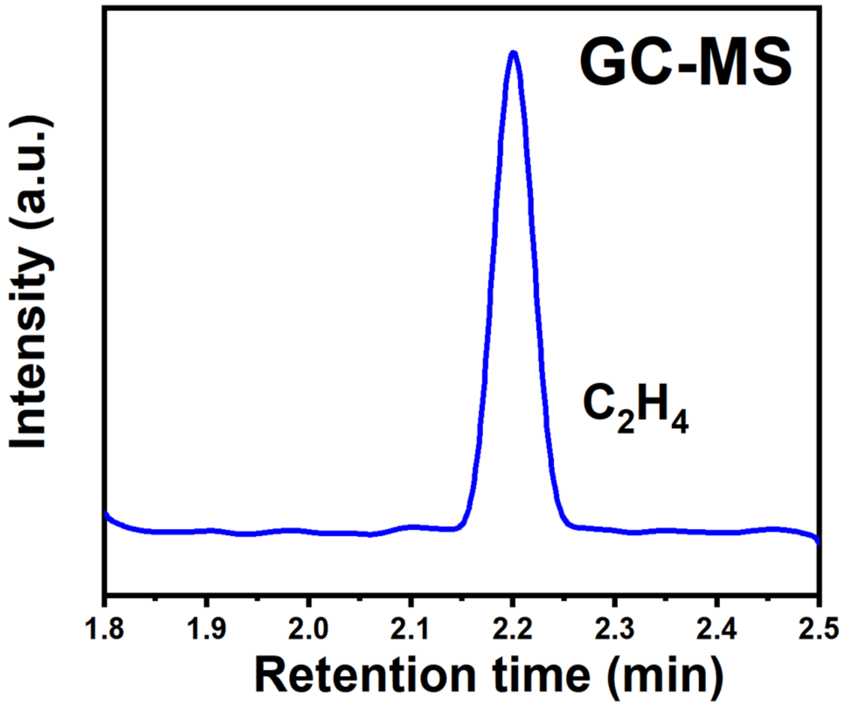

Fig. S11 The isotope analysis of $^{13}C_2H_4$ using $^{13}CO_2$ as carbon source by GC-MS.

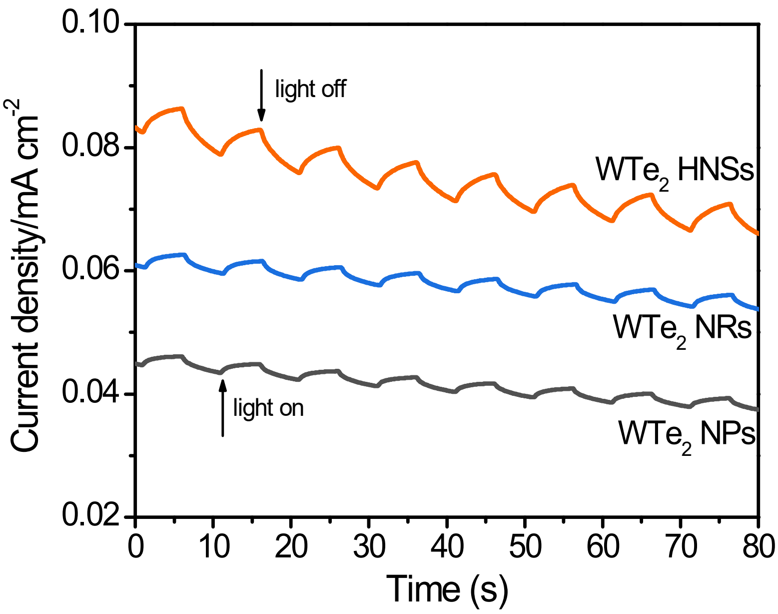

Fig. S12 Photocurrent density measured in 0.5 M KPi buffer solution (pH=7) at open-circuit voltage under AM 1.5 G illumination.

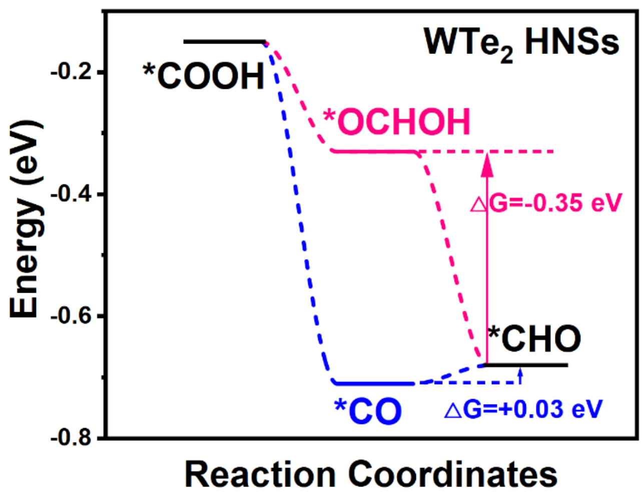

Fig. S13 Speed steps of two kinds of possible *COOH-*CHO pathways over WTe_2 HNSs.

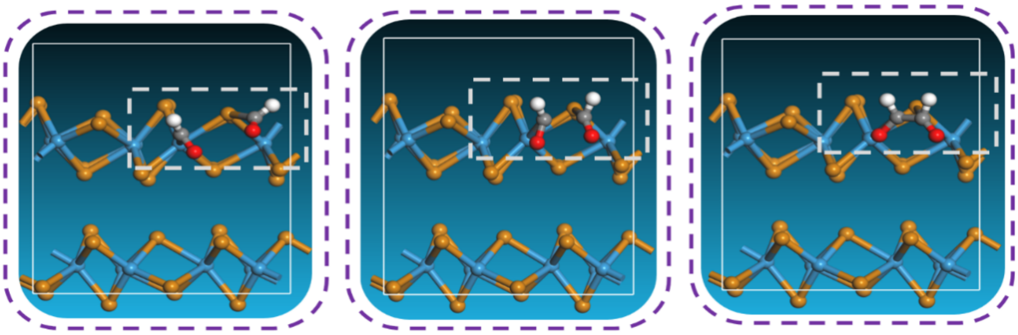

Fig. S14 The structures of the initial states, transition states and final states for CO_2 photothermal catalytic reduction to C_2H_4 on a WTe_2 HNSs surface (blue spheres = W, orange spheres = Te, red spheres = O, gray spheres = C and white spheres = H).

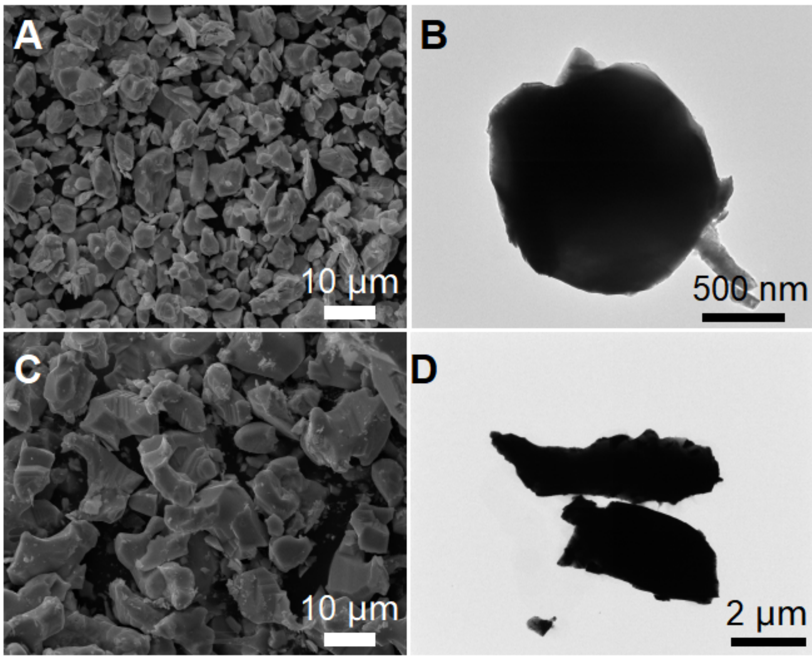

Fig. S15 FE-SEM image of (a) $PtTe_2$ and (c) NiTe; the whole TEM image of (b) $PtTe_2$ and (d) NiTe.

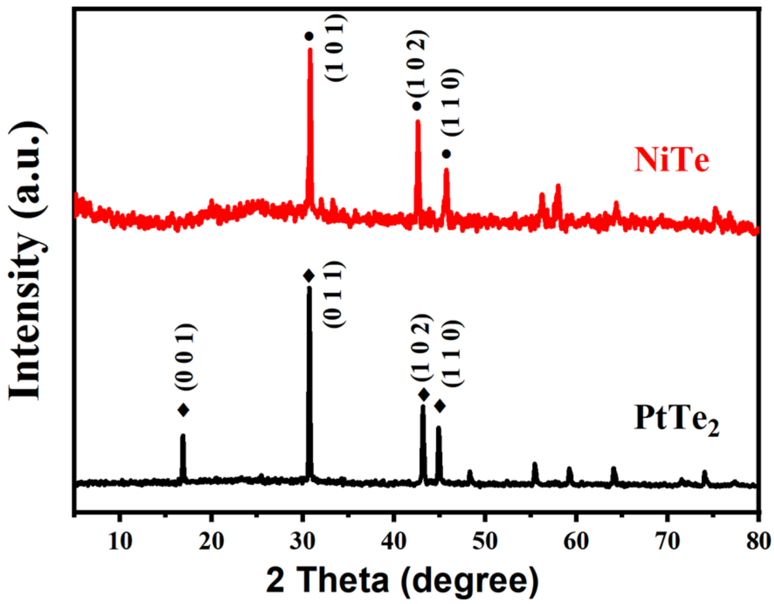

Fig. S16 XRD patterns of $PtTe_2$ and NiTe.

Table S1. Performance comparison of WTe_2 and recently reported photothermal catalysts for C_{2+} production.

Catalyst	Feeds (CO_2 + H_2O/H_2)	light source	C_{2+} (μmol/g)	C_{2+} sel.%
Ni, Co-doped BZCY532[1]	CO_2+H_2O	300W Xe lamp	C_2H_6= 8.64 μmol/g C_3H_8=3.22 μmol/g	C_2H_6=17% C_3H_8=7%
$CoMn_x/(MnO_2)_{2-X}$ [2]	CO/H_2/Ar =20/20/60	300W Xe lamp	CO conversion:13.9%	32.4%
WO_{3-X}[3]	CO_2+H_2O	300W Xe lamp	C_2H_4=5.3 μmol/g C_2H_6=0.93 μmol/g	>34%
CoAl-LDH(700)[4]	CO/H_2/Ar =20/60/20	300W Xe lamp	CO conversion: 35.4%	36.3%
CoFe-650[5]	CO_2/H_2/Ar =15/60/25	300W Xe lamp	CO_2 conversion: 82.2%	36.42%
Co/Co_3O_4[6]	CO/H_2/Ar =20/60/20	300W Xe lamp	CO conversion: 15.4%	41.9%
NiO_X/Nb_2O_5[7]	CO_2+H_2	UV irradiation	C_2H_6=194.18 μmol/g	C_2H_6=57.5%
Ni-500[8]	CO/H_2/Ar =20/60/20	300W Xe lamp	CO conversion: 15 %	65.1%
WTe_2 NPs This work	**CO_2+H_2O**	**300W Xe lamp**	**C_2H_4=41.6 μmol/g**	**C_2H_4=82%**

WTe_2 NRs **This work**	**CO_2+H_2O**	**300W** **Xe lamp**	**C_2H_4=87.7 µmol/g**	**C_2H_4=87%**
WTe_2 HNSs **This work**	**CO_2+H_2O**	**300W** **Xe lamp**	**C_2H_4=115.5** **µmol/g**	**C_2H_4=88%**

Supporting Reference

1. J. Tian, Y. Ren, L. Liu, Q. Guo, N. Sha, Z. Zhao, *Mater. Res. Express*, 2020, **7**, 085504.
2. R. Li, Y. Li, Z. Li, W. Wei, S. Ouyang, H. Yuan, T. Zhang, *Sol. RRL*, 2020, **11**, 2000488.
3. Y. Deng, J. Li, R. Zhang, C. Han, Y. Chen, Y. Zhou, W. Liu, P. K. Wong, L. Ye, *Chinese J. Catal.*, 2022, **43**, 1230-1237.
4. Z. Li, J. Liu, Y. Zhao, R. Shi, G. I. N. Waterhouse, Y. Wang, L. Wu, C. H. Tung, T, Zhang, *Nano Energy*, 2019, **60**, 467-475.
5. G. Chen, R. Gao, Y. Zhao, Z. Li, G. I. N. Waterhouse, R. Shi, J. Zhao, M. Zhang, L. Shang, G. Sheng, X. Zhang, X. Wen, L. Wu, C. H. Tung, T. Zhang, *Adv. Mater.*, 2018, **30**, 1704663.
6. Z. Li, J. Liu, Y. Zhao, G. I. N. Waterhouse, G. Chen, R. Shi, X. Zhang, X. Liu, Y. Wei, X. Wen, L. Wu, C. H. Tung, T. Zhang, *Adv. Mater.*, 2018, **30**, 1800527.
7. Z. Wang, M. Xiao, X. Wang, H. Wang, X. Chen, W. Dai, Y. Yu, X. Fu, *Appl. Surf. Sci.*, 2022, **592**, 153246.
8. Y. Wang, Y. Zhao, J. Liu, Z. Li, G. I. N. Waterhouse, R. Shi, X. Wen, T. Zhang, *Adv. Energy Mater.,* 2020, **10**, 1902860.